LBNL-47750
Preprint

ERNEST ORLANDO LAWRENCE BERKELEY NATIONAL LABORATORY

CP-Violation from Noncommutative Geometry

I. Hinchliffe and N. Kersting

Physics Division

April 2001

Submitted to
Physical Review D

REFERENCE COPY
Does Not
Circulate
Library Annex Reference
Lawrence Berkeley National Laboratory
Copy 1
LBNL-47750

DISCLAIMER

This document was prepared as an account of work sponsored by the United States Government. While this document is believed to contain correct information, neither the United States Government nor any agency thereof, nor the Regents of the University of California, nor any of their employees, makes any warranty, express or implied, or assumes any legal responsibility for the accuracy, completeness, or usefulness of any information, apparatus, product, or process disclosed, or represents that its use would not infringe privately owned rights. Reference herein to any specific commercial product, process, or service by its trade name, trademark, manufacturer, or otherwise, does not necessarily constitute or imply its endorsement, recommendation, or favoring by the United States Government or any agency thereof, or the Regents of the University of California. The views and opinions of authors expressed herein do not necessarily state or reflect those of the United States Government or any agency thereof or the Regents of the University of California.

LBNL-47750

CP-violation from Noncommutative Geometry*

I. Hinchliffe and N. Kersting
Lawrence Berkeley National Laboratory, Berkeley, CA

Abstract

If the geometry of space-time is noncommutative, *i.e.* $[x_\mu, x_\nu] = i\theta_{\mu\nu}$, then noncommutative CP violating effects may be manifest at low energies. For a noncommutative scale $\Lambda \equiv \theta^{-1/2} \leq 2\ TeV$, CP violation from noncommutative geometry is comparable to that from the Standard Model (SM) alone: the noncommutative contributions to ϵ and ϵ'/ϵ in the K-system, and to $sin\ 2\beta$ in the B-system, may actually dominate over the Standard Model contributions. Present data permit noncommutative geometry to be the only source of CP violation. Furthermore the most recent findings for $g-2$ of the muon are consistent with predictions from noncommutative geometry.

Contents

1 Introduction 1

2 Computing in the Noncommutative Standard Model(ncSM) 2

3 CP Violation in the ncSM 4
- 3.1 CP Violating Observables . . . 5
  - 3.1.1 ϵ_K . . . 5
  - 3.1.2 ϵ'/ϵ . . . 6
  - 3.1.3 $sin2\beta$ and the unitarity triangle . . . 7
  - 3.1.4 Electric Dipole Moments . . . 8

4 Constraints from g − 2 of the Muon 9

5 Conclusions 11

A Feynman Rules in the NCSM 12

B Kaon System 13

C ϵ'/ϵ 13

D $g-2$ of the muon 14

*This work was supported in part by the Director, Office of Science, Office of High Energy and Nuclear Physics, of the U.S. Department of Energy under Contract DE-AC03-76SF00098.

1 Introduction

In recent years there has been a growing interest in quantum field theory over noncommutative spaces [1], that is spaces where the space-time coordinates x_μ, replaced by hermitian operators $\widehat{x}_\mu$, do not commute:

$$[\widehat{x}_\mu, \widehat{x}_\nu] = i\theta_{\mu\nu} \tag{1}$$

Here θ is a real and antisymmetric object with the dimensions of length-squared and corresponds to the smallest patch of area in physical space one may 'observe', similar to the role $\hbar$ plays in $[\widehat{x}_i, \widehat{p}_j] = i\hbar\delta_{ij}$, defining the corresponding smallest patch of phase space in quantum mechanics. In this paper we define the energy scale $\Lambda \equiv \frac{1}{\sqrt{\theta}}$ (where θ is the average magnitude of an element of $\theta_{\mu\nu}$) which is a more convenient parameterization in constructing an effective theory at low energies. Many researchers set $\theta_{0i} = 0$ to avoid problems with unitarity and causality, but since this is only an issue at energies above Λ [2], we do not use this constraint for the purposes of low-energy phenomenology. We may view $\theta_{\mu\nu}$ as a "background B-field" which has attained a vacuum expectation value, hence appearing in the Lagrangian as a Lorentz tensor of constants [3]. Assuming that the components of $\theta_{\mu\nu}$ are constant over cosmological scales, in any given frame of reference there is a special "noncommutative direction" given by the vector $\theta^i \equiv \epsilon^{ijk}\theta_{jk}$. Experiments sensitive to noncommutative geometry will therefore be measuring the components of $\overrightarrow{\theta}$, and it is necessary to take into account the motion of the lab frame in this measurement. Since noncommutative effects are measured in powers of $p^\mu\theta_{\mu\nu}p'^\nu$, where p, p' are some momenta involved in the measurement, it is possible that odd powers of θ will partially average to zero if the time scale of the measurement is long enough. Effects of first order in θ vanish at a symmetric e^+e^--collider, for example, if the measurement averages over the entire 4π solid angle of decay products. If the data is binned by angle then it is possible to restore the sensitivity to θ. In addition to any other averaging process over short time scales, terrestrial experiments performed over several days will only be sensitive to the projection of $\overrightarrow{\theta}$ on the axis of the Earth's rotation. Of course binning the data hourly or at least by day/night, taking into account the time of year, can partially mitigate this effect. This axis, as well as the motion of the solar system, galaxy, *etc.*, does not vary over time scales relevant to terrestrial experiments.

The basic idea of noncommutative geometry is not new and has been known in the context of string theory for some time [4]. We refer the reader to a few of the many excellent reviews of the mathematics of noncommutative space [5, 6, 7, 8, 9] for a more rigorous understanding of the present material. Noncommuting coordinates are expected on quite general grounds in any theory that seeks to incorporate gravity into a quantum field theory: the usual semi-classical argument is that a particle may only be localized to within a Planck length λ_P without creating a black hole that swallows the particle, hence $\sum_{i<j} \Delta x_i \Delta x_j \geq {\lambda_P}^2$; alternatively, one is led to think of space as a noncommutative algebra upon trying to quantize the Einstein theory [10, 11].

Much research has already gone into understanding noncommutative quantum field theory [12, 13, 14, 15]; it is equivalent to working with ordinary (commutative) field theory and replacing the usual product by the $\star$ product defined as follows:

$$(f \star g)(x) \equiv e^{i\theta_{\mu\nu}\partial^y_\mu \partial^z_\nu} f(y)g(z) \mid_{y=z=x} \tag{2}$$

With this definition (1) holds in function space equipped with a $\star$ product:

$$[x_\mu, x_\nu]_\star = i\theta_{\mu\nu} \tag{3}$$

This $\star$ product intuitively replaces the point-by-point multiplication of two fields by a sort of 'smeared' product (see Fig. 1). Indeed the concept of 'smearing' is borne out in more detailed

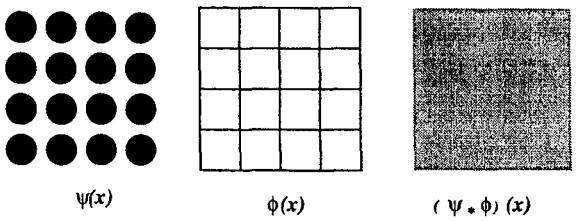

Figure 1: An illustration of the star product between two functions. The two scalar functions ψ and ϕ are strongly orthogonal($\psi(x)\phi(x) = 0 \ \ \forall x$) yet the $\star$ product is nonzero.

analysis of 1- and 2- point functions [16]: spacetime is only well defined down to distances of order $\sqrt{\theta}$ so functions of spacetime must be appropriately averaged over a neighborhood of points. In each (i, j) plane, we must replace

$$\phi(x_i, x_j) \to \int dx'_i dx'_j \phi(x') e^{-\frac{(x_i - x'_i)^2 + (x_j - x'_j)^2}{\theta_{ij}}} (\pi\theta_{ij})^{-1} \tag{4}$$

Examples of theories which have received attention include scalar field theory [13, 17, 18], NC-QED (the noncommutative analog of QED) [19], as well as noncommutative Yang-Mills [20, 21]; perturbation theory in θ is applicable and the theories are renormalizable [22, 23]. For gauge theories, the most naive possibility of a gauge transformation only permits $U(N)$ gauge groups with a severely limited choice of particle representations [19]; NCQED for example would only permit particles with charges $+1, 0, -1$, while color $SU(3)$ would be forbidden altogether in a noncommutative framework. With a more suitable treatment of the gauge transformations however [24], such limitations are removed†. A noncommutative modification of the Standard Model(SM) is possible as a working field theory, at least up to $\mathcal{O}(\theta)$. Replacing the ordinary product with the $\star$ product in the Lagrangian, the appropriate Feynman rules for this noncommutative SM (ncSM) follow straightforwardly and are reproduced in the Appendix.

Whatever the physics at the Planck scale is like, we expect there to be some residual effect at low energies beyond that of classical gravity. If we parameterize this effect as in (1), then low energy physics will receive corrections in powers of the small parameter θ. Several papers have addressed how these corrections may modify observations at an accelerator [25], precision tests of QED in hydrogen [26], and various dipole moments [27]; in general, if $\Lambda \leq 1\ TeV$, there will be some observable effects in these systems at the next generation of colliders. This paper aims to investigate the CP violating potential of noncommutative geometry in low energy phenomenology.

2 Computing in the Noncommutative Standard Model(ncSM)

The method of computing noncommutative field theory amplitudes is effected by replacing the ordinary function product with the $\star$ product in the Lagrangian. The theory is otherwise identical to the commuting one (i.e. the Feynman path integral formulation provides the usual setting for doing QFT): for example a Yukawa theory with a scalar ϕ, Dirac fermion ψ, has the action

$$S = \int d^4x \left(\overline{\psi} i \partial\!\!\!/ \psi + (\partial\phi)^2 + \lambda \overline{\psi} \star \psi \star \phi \right) \tag{5}$$

†the most naive gauge transformation is $\delta\phi(x) = \alpha(x)^a \star T_a \phi(x)$, the $\mathcal{O}(\theta)$ piece of which causes the aforementioned difficulties. Since we only work to $\mathcal{O}(\theta)$ in this paper, we could for example use instead $\delta\phi(x) = \alpha(x)^a \star \overrightarrow{T_a}\phi(x) + \phi(x)\overleftarrow{T_a} \star \alpha(x)^a$ which is $\mathcal{O}(1 + \theta^2)$

(Here we have used the fact that $\int dx\xi \star \xi = \int dx\xi\xi$, which follows straightforwardly from (2)) Gauge interactions likewise generalize from the standard form; the action for NCQED for example is

$$S = \int d^4x \left(-\frac{1}{4e^2} F^{\mu\nu} F_{\mu\nu} + \overline{\psi} i \partial\!\!\!/ \psi - e\overline{\psi} \star A\!\!\!/ \star \psi - m\overline{\psi}\psi \right) \tag{6}$$

where

$$F_{\mu\nu} \equiv \partial_\mu A_\nu - \partial_\nu A_\mu - i[A_\mu, A_\nu]_\star \tag{7}$$

Note the extra term in the field strength which is absent in ordinary QED; this nonlinearity gives NCQED a NonAbelian-like structure. There will be, for example, 3- and 4-point photon self-couplings at tree level (see Appendix).

In momentum space the $\star$ product becomes a momentum-dependent phase factor which means that the theory effectively contains an infinite number of derivative interactions suppressed by powers of θ. This directly exhibits the nonlocal character of noncommutative geometry. From (5) and (6) we can derive the action for the noncommutative version of the Standard Model (ncSM). We present its content as the list of Feynman rules in the Appendix.

A central feature of computations in the SM is the presence of divergences and the need to absorb them into counterterms. The ncSM is similar in this respect, yet it is necessary to renormalize carefully: if one simply uses dimensional regularization and sums virtual energies to infinity, bizarre infrared singularities appear in the theory which are difficult to handle [13]. To illustrate, consider the loop integral

$$\int d^d k \frac{e^{ik^\mu \theta_{\mu\nu} p^\nu}}{(k^2 - m^2)^2} \tag{8}$$

which is finite for $|\theta \cdot p| \neq 0$ but is logarithmically divergent if $|\theta| = 0$. Explicitly, we Wick-rotate (8), introduce the Schwinger parameters [28], integrate over momenta, and obtain

$$\int dS\ S^{1-\frac{d}{2}}\ e^{-\frac{1}{4}(\theta\cdot p)^2 S^{-1} - m^2 S} \tag{9}$$

If we take $|\theta| = 0$ now, dimensional regularization gives the usual $\Gamma[1 - \frac{d}{2}]$ which we would absorb into a counterterm of the theory. However for small finite values of $|\theta \cdot p|$ we get an approximation of the integral (9) in four dimensions:

$$\int d^4 k \frac{e^{ik^\mu \theta_{\mu\nu} p^\nu}}{(k^2 - m^2)^2} \approx ln(m^2 \left|\theta \cdot p\right|^2) \left(1 + m^2 \left|\theta \cdot p\right|^2\right) \tag{10}$$

There is a $ln(|\theta|)$ divergence as $|\theta| \to 0$ which is expected since in this limit the theory tends to the commutative one and reproduces the $\Gamma[1 - \frac{d}{2}]$ divergence mentioned above. This is formally correct, however the theory in this limit is awkward to work with since some amplitudes will diverge as $|\theta| \to 0$ and must somehow conspire to produce final results such as scattering amplitudes which are finite. For the computational purposes of this paper, in which *e.g.* ${m_W}^2 \left|\theta\right|$ is a small number $\ll 1$, it is more convenient to regularize with a Pauli-Vilars regulator whose cutoff M satisfies $M \sim \mathcal{O}(\Lambda)$. Then (9) becomes

$$\int dS\ S^{1-\frac{d}{2}}\ e^{-(M^{-2} + \frac{1}{4}(\theta\cdot p)^2) S^{-1} - m^2 S} \tag{11}$$

Now taking the limit $|\theta| \to 0$ also raises the Pauli-Vilars scale M and

$$\int d^d k \frac{e^{ik^\mu \theta_{\mu\nu} p^\nu}}{(k^2 - m^2)^2} \approx ln(\frac{m^2}{M^2} + m^2 \left|\theta \cdot p\right|^2) \left(1 + m^2 \left|\theta \cdot p\right|^2\right) \tag{12}$$

The divergent log piece $\sim ln(M^2)$ can be subtracted in a counterterm while the second, finite piece $\sim |\theta \cdot p|^2 ln(M^2)$ gives a small correction to the commutative theory of $\mathcal{O}(x\, ln(x))$ where $x \equiv |\theta \cdot p|^2$. Renormalizing in this manner guarantees sensible amplitudes as well as physical results.

3 CP Violation in the ncSM

In the SM, there are only two sources of CP violation: the irremovable phases in the CKM matrix and the $\Theta F\tilde{F}$ term in the strong interaction Lagrangian(the coefficient Θ has to be miniscule to avoid contradicting experiment [29]).

In the ncSM, there is an additional source of CP violation: the parameter θ itself is the CP violating object, which is apparent from the NCQED action (6) considering the transformation of A_μ and ∂_μ under C and P and assuming CPT invariance [30]. Physically speaking, an area of $\mathcal{O}(\theta)$ represents a "black box" in which some or all spacetime coordinates become ambiguous, which in turn leads to an ambiguity between particle and antiparticle. More detailed work reveals that θ is in fact proportional to the size of an effective particle dipole moment [31]. Therefore noncommutative geometry can actually *explain* the origin of CP violation. At the field theory level, it is the momentum-dependent phase factor appearing in the noncommutative theory which gives CP violation. For example, the ncSM W-quark-quark $SU(2)$ vertex in the flavor basis is

$$\mathcal{L}_{Wqq} = \overline{u(p)}\gamma^\mu(1-\gamma_5)e^{ip\cdot\theta\cdot p'}\; d(p')\; W_\mu \qquad (13)$$

Once we perform rotations on the quark fields to diagonalize the Yukawa interactions, *i.e.* $u_L \to Uu_L$ and $d_L \to Vd_L$, the above becomes

$$\mathcal{L}_{Wqq} = \overline{u(p)}\gamma^\mu(1-\gamma_5)e^{ip\cdot\theta\cdot p'}U^\dagger V\; d(p')\; W_\mu \qquad (14)$$

Even if $U^\dagger V$ is purely real, there will be some nonzero phases $e^{ip\cdot\theta\cdot p'}$ in the Lagrangian whose magnitudes increase as the momentum flow in the process increases.

Experimentally, the signal for noncommutative geometry here is a momentum-dependent CKM matrix (ncCKM) which we define as follows:

$$\overline{V}(p,p') \equiv \begin{pmatrix} 1-\lambda^2/2+ix_{ud} & \lambda+ix_{us} & A\lambda^3(\rho-i\eta)+ix_{ub} \\ -\lambda+ix_{cd} & 1-\lambda^2/2+ix_{cs} & A\lambda^2+ix_{cb} \\ A\lambda^3(1-\rho-i\eta)+ix_{td} & -A\lambda^2+ix_{ts} & 1+ix_{tb} \end{pmatrix} \qquad (15)$$

where $x_{ab} \equiv {p_a}^\mu \theta_{\mu\nu} {p'_b}^\nu$ for quarks a, b. This matrix is an approximation of the exact ncSM in the perturbative limit where we expand $e^{ip\cdot\theta\cdot p'} \approx 1 + ip\cdot\theta\cdot p'$. In the limit $\theta \to 0$, the x_{ab} all go to zero and $\overline{V}$ becomes the CKM matrix V in the Wolfenstein parameterization [32] in terms of the small number $\lambda \approx 0.22$. Note that $\overline{V}$ is not guaranteed to be unitary, since, in contrast to the SM CKM matrix, $\overline{V}$ is not a collection of derived constants: a given matrix element will attain different values depending on the process it is describing. As an example, suppose we measure a non-zero τ-polarization asymmetry in $t \to b\tau^+\nu$ [33]; this puts a constraint on the value of $\Im(\overline{V}_{tb})$ *at the energy scale* $\mu \approx m_t$[‡]. We can get another constraint on $\Im(\overline{V}_{tb})$ through a $B^0 - \overline{B}^0$ oscillation experiment, but we must take into consideration that this is a measurement at the energy scale $\mu \approx m_b$. In the former process we would find (for $\eta = 0$) $\Im(\overline{V}_{tb}) \approx \mathcal{O}({m_t}^2\,|\theta|)$ whereas in the latter it would be $\mathcal{O}(m_t m_b\,|\theta|)$, so these phases differ by a factor of $m_t/m_b \approx 30$. Therefore we expect the

[‡]Actually, there is a lot of uncertainty in this measurement, including the values of the MNS matrix, so measuring the phase in practice is not straightforward.

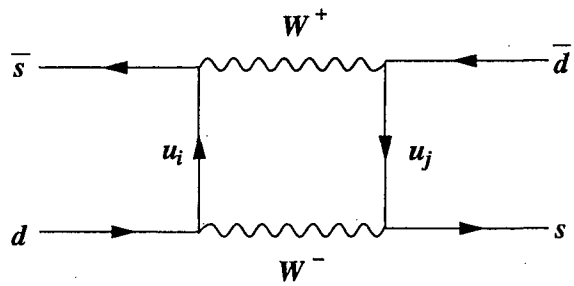

Figure 2: The box graph for K^0-$\overline{K^0}$ mixing in the Standard Model with exchange of virtual W-bosons and up-type quarks from the i, j generations.

phenomenology of $\overline{V}$ to be rather different from that of the SM. In addition to CP violation from the weak interaction (in $\overline{V}$), there will also be CP violation from the strong and electromagnetic interactions (since there are phases entering any vertex with three (or more) fields (see Appendix)). We now turn to the phenomenological implications of these.

3.1 CP Violating Observables

3.1.1 ϵ_K

The CP violating observable of choice in the K^0-meson system is ϵ_K which is directly proportional to the imaginary part $\Im(M_{12})$ of the box graph (see Fig. 2):

$$\epsilon_K \equiv \frac{\Im(M_{12})}{\Delta m} \tag{16}$$

The mass splitting Δm between the long- and short-lived K^0 eigenstates is $\Delta m \approx 3.5 \cdot 10^{-15}\ GeV$ [34]. We can rewrite

$$\Im(M_{12}) = \frac{{G_F}^2 {m_W}^2 {f_K}^2 B_K m_K}{12\pi^2} \Im(loop) \tag{17}$$

in terms of the decay constants f_K, B_K, and the loop factor. In the SM, the loop factor is

$$\Im(loop) \approx \Im({\lambda_c}^2 f(m_c) + {\lambda_t}^2 f(m_t) + \lambda_c \lambda_t f(m_c, m_t)) \tag{18}$$

where $\lambda_q \equiv V_{qd} V_{qs}^*$ and $f(x)$ is a loop function (see Appendix). In the SM, both charm and top quarks contribute roughly equally to the imaginary part of the loop, and the measured value for ϵ_K puts a constraint on the parameters ρ, η of the CKM matrix. However, in the ncSM we must replace the entire loop since the momentum-dependent phases in $\overline{V}$ change how the loop integral behaves. The top-quark will dominate the graph because of the large loop momentum it carries. We record the evaluation of the loop integral in the Appendix.

If the kaons used in the measurement emerge from a beam with an average velocity $\beta \equiv \frac{v}{c}$ in the lab frame, we must average over the motion of the internal constituents of the kaon, since the entire noncommutative effect is proportional to $p \cdot \theta \cdot p'$, where p, p' are the momenta of the constituents. We assume that these momenta have random orientation in the rest frame of the kaon, subject to $p + p' = (m_K, 0, 0, 0)$. The average over these internal momenta produces a result which is proportional to the velocity of the kaon in the lab frame: $\langle p \cdot \theta \cdot p' \rangle \approx |\theta| \beta\gamma\ m_K^2$. Therefore it is important that the $\beta\gamma$ of the beam not be so small as to wash out the signal. Recent determinations

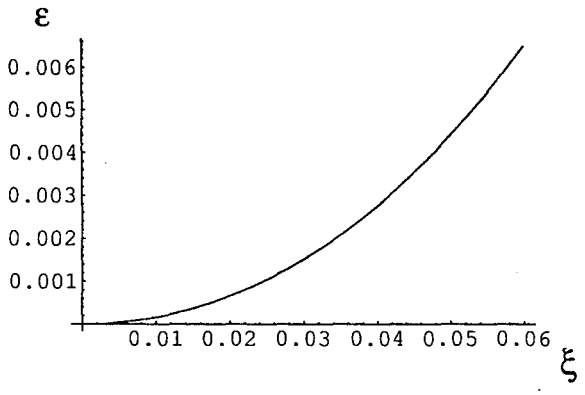

Figure 3: Variation of ϵ with $\xi \equiv m_W/\Lambda$. Here $\eta = 0$ so all CP violation is from noncommutative geometry.

of ϵ_K use a reasonable $\beta\gamma$ [35], so we do not concern ourselves further with this caveat. Experiments at an e^+e^- collider (*e.g.* [36, 37]) where the center of mass is stationary in the lab frame should, however, see no signal for ϵ_K since $\langle \vec{\beta}\gamma \rangle = 0$. As we mentioned in the Introduction, the data is sensitive to the time of day. If there is a component of $\vec{\theta}$ along the axis of the Earth, then given enough statistics there should be a "day/night effect" for ϵ_K which, as far as we know, no experiment has looked for.

In the case $\eta = 0$ (so the phase from $\overline{V}$ is due entirely to noncommutative geometry), we obtain

$$\begin{aligned} \epsilon_K &\approx \tfrac{G_F{}^2 m_W{}^2 f_K{}^2 B_K m_K}{12\pi^2 \Delta m} F(\xi) \\ F(\xi) &\equiv \tfrac{m_K}{18 m_W} \lambda^3 \rho \left(\tfrac{29\pi}{2}\xi^2 + \tfrac{134\xi^3}{1+\xi^2} - \tfrac{20\xi^3}{4+\xi^2} \right) \\ \xi &\equiv \tfrac{m_W}{\Lambda} \end{aligned} \tag{19}$$

Using $G_F = 1.166 \cdot 10^{-5}\ GeV^{-2}, m_W = 80.4\ GeV, f_K = 0.16\ GeV, m_K = 0.498\ GeV, B_K = 0.70 \pm 0.2, \rho = 0.3 \pm 0.2$, and the latest measurement of $\epsilon_K \approx (2.280 \pm 0.013) \cdot 10^{-3}$ [34], this implies $\xi \approx (4 \pm 2) \cdot 10^{-2}$ (see Fig. 3); in this scenario spacetime becomes effectively noncommutative at energies above $\approx 2\ TeV$.

3.1.2 ϵ'/ϵ

Direct CP violation is measurable in the neutral kaon system as a difference between the rates at which $K_{L,S}$ decay into $I = 0, 2$ states of pions:

$$\epsilon' \equiv \frac{\langle 2 \mid T \mid K_L \rangle \langle 0 \mid T \mid K_S \rangle - \langle 2 \mid T \mid K_S \rangle \langle 0 \mid T \mid K_L \rangle}{\sqrt{2} \langle 0 \mid T \mid K_S \rangle^2} \tag{20}$$

Then the ratio of direct to indirect CP violation is

$$\frac{\epsilon'}{\epsilon} = \frac{1}{\sqrt{2}} \left(\frac{\langle 2 \mid T \mid K_L \rangle}{\langle 0 \mid T \mid K_L \rangle} - \frac{\langle 2 \mid T \mid K_S \rangle}{\langle 0 \mid T \mid K_S \rangle} \right) \tag{21}$$

The theoretical computation of this ratio is a challenge in the SM not only because the perturbative description of the strong interaction is not reliable at low energies but also because it is proportional

to a difference between two nearly equal types of contributions, enhancing the theoretical error [38]. The most naive way to estimate $\frac{\epsilon'}{\epsilon}$ employs the so-called vacuum-saturation-approximation (VSA) which is based on the factorization of four-quark operators into products of currents and the use of the vacuum as an intermediate state (for more details see [39]). The estimate is

$$\frac{\epsilon'}{\epsilon} \approx (0.8 \pm 0.5) \cdot 10^{-3} \left(\frac{\Im(\lambda_t)}{10^{-4}}\right) \tag{22}$$

where in the SM λ_t represents the CP violating phases from the CKM matrix, $\lambda_t = A^2\lambda^5\eta \approx 1.3 \cdot 10^{-4}$. The experiments measure $\frac{\epsilon'}{\epsilon} = (1.92 \pm 0.46) \cdot 10^{-3}$ which does not closely match the VSA number, but it is possible to use more elaborate models that agree closely with the measured value [38].

In the ncSM it is no less difficult to compute $\frac{\epsilon'}{\epsilon}$; in particular, the extra phases from noncommutative geometry will become involved in the complicated nonperturbative quark-gluon dynamics. The best estimate we can make here is (see Appendix C)

$$\Im(\lambda_t) \approx 2\frac{m_K}{m_W}\xi^2 \; ln(\frac{m_W}{\xi m_K}) \tag{23}$$

For $\xi \approx 0.04$, we get roughly the same VSA value as in the SM.

3.1.3 $sin2\beta$ and the unitarity triangle

The only CP violating observation from the B-system to date, the asymmetry in the decay products of $B^0 \to J/\psi K_s{}^0$ [40, 41, 42, 43], is a measurement in the SM of a combination of CKM elements called $sin2\beta$:

$$sin2\beta \equiv \Im\left(-\left[\frac{V_{tb}^* V_{td}}{V_{tb}V_{td}^*}\right]\left[\frac{V_{cs}^* V_{cb}}{V_{cs}V_{cb}^*}\right]\left[\frac{V_{cd}^* V_{cs}}{V_{cd}V_{cs}^*}\right]\right) \tag{24}$$

where the first bracketed factor is from $B_d{}^0 - \overline{B_d}^0$ mixing, the second from the observed decay asymmetry, and the third from $K^0 - \overline{K}^0$ mixing. In the Wolfenstein parameterization,

$$sin2\beta \approx \frac{2\eta(1-\rho)}{\eta^2 + (1-\rho)^2} \tag{25}$$

which, for $(\rho, \eta) \approx (0.2, 0.3)$, corresponding to a point in the center of the allowed region of the $\rho - \eta$ plane [44] implies $sin2\beta \approx 0.7$. The most recent experimental world average for this quantity is $\approx 0.49 \pm 0.23$ [45], which may suggest that the SM does not adequately account for the observed CP violation.

In the ncSM the corresponding quantity is (24) with each matrix element V_{ij} replaced by $\overline{V}_{ij}$ extracted from the relevant process:

$$sin2\beta \to \Im\left(-\left[\frac{\overline{V}_{tb}^* \overline{V}_{td}}{\overline{V}_{tb}\overline{V}_{td}^*}\right]\left[\frac{\overline{V}_{cs}^* \overline{V}_{cb}}{\overline{V}_{cs}\overline{V}_{cb}^*}\right]\left[\frac{\overline{V}_{cd}^* \overline{V}_{cs}}{\overline{V}_{cd}\overline{V}_{cs}^*}\right]\right) \tag{26}$$

Of course experiments don't measure the precise value of a given $\overline{V}_{ij}$ but rather some combination of them integrated over internal momenta. If we again consider the scenario where $\eta = 0$ then the imaginary parts of these quantities increase roughly proportionally to the momentum involved and we expect the first bracketed term in (26) to dominate since the size of the momenta involved in

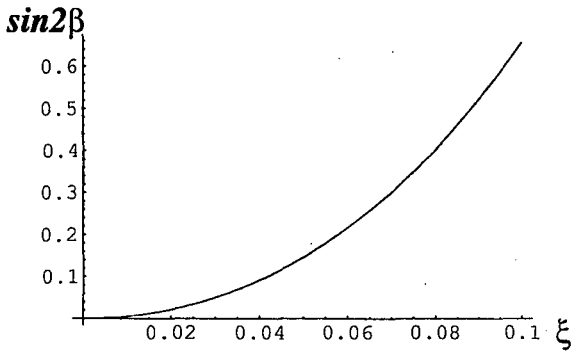

Figure 4: Variation of $sin2\beta$ with $\xi \equiv m_W/\Lambda$ ($\eta = 0$). Consistency with K-system measurements implies $\xi \approx 0.04 \pm 0.02$, so the ncSM predicts a small $sin2\beta \approx 0.11 \pm 0.08$

${B_d}^0 - \overline{B_d}^0$ mixing exceeds that of B^0-decay or $K^0 - \overline{K}^0$ mixing, *i.e.* $m_b m_t \theta \gg m_b^2\theta, m_K m_t \theta$. We therefore set the second and third brackets to unity, obtaining

$$\begin{aligned} sin2\beta &\approx \Im\left(\frac{\lambda^3(1-\rho)+if(\xi)}{\lambda^3(1-\rho)-if(\xi)}\right) \approx \frac{2f(\xi)}{\lambda^3(1-\rho)} \\ f(\xi) &\equiv \frac{m_B}{m_K\lambda^3\rho}F(\xi) \qquad \text{see(19)} \end{aligned} \tag{27}$$

The motion of the quarks inside the B-meson would be a serious impediment to measuring θ (see previous discussion for kaons) were it not for the asymmetry of the e^+e^- collider which gives the ${B_d}^0 - \overline{B_d}^0$ center-of-mass a boost of $\beta\gamma \approx 0.6$ in the lab frame, providing the dominant contribution to the quarks' motion. In Figure 4 we plot $sin2\beta$ in the ncSM for a range of $\xi \equiv m_W/\Lambda$. If we use the measurement of ϵ_K to fix ξ, then the ncSM predicts $sin2\beta \approx 0.11 \pm 0.08$ which is consistent with experiment.

The other two CP violating observables commonly defined in B-physics are α and γ:

$$\alpha \equiv arg\left(-\frac{V_{tb}^* V_{td}}{V_{ud}V_{ub}^*}\right) \qquad \gamma \equiv arg\left(-\frac{V_{cd}^* V_{cb}}{V_{td}V_{tb}^*}\right) \tag{28}$$

where $V_{tb}^* V_{td}$ is extracted from ${B_d}^0 - \overline{B_d}^0$ mixing and $V_{ud}V_{ub}^*$, $V_{cd}^* V_{cb}$ from B^0-decays to $\pi\pi$ and KD, respectively. In the SM $\alpha + \beta + \gamma = \pi$ because the CKM matrix V is unitary. The ncSM matrix $\overline{V}$ is not unitary (see Section 3), so we expect $\alpha + \beta + \gamma \neq \pi$ as these "angles" are defined (by $\overline{V}$ replacing V in (28) above). For $\eta = 0$ the parameters α, β, γ in the ncSM assume the following form:

$$\begin{aligned} \alpha &= tan^{-1}\left(\frac{1}{\lambda^3\rho}\frac{m_b^2}{m_W^2}\xi^2 + \frac{1}{\lambda^3}f(\xi)\right) \\ \beta &= tan^{-1}\left(\frac{1}{\lambda^3(1-\rho)}f(\xi)\right) \\ \gamma &= tan^{-1}\left(\frac{1+\rho}{\lambda^3\rho}\frac{m_b^2}{m_W^2}\xi^2\right) \end{aligned} \tag{29}$$

In Figure 5 we plot the sum $\alpha + \beta + \gamma$. The angles clearly do not add up to π in the same range of ξ which is required by the ϵ_K-constraint.

3.1.4 Electric Dipole Moments

Nonzero values of the electric dipole moments (*edms*) of the elementary fermions necessarily violate T, and hence CP (assuming the CPT theorem). This follows from the observation that a dipole

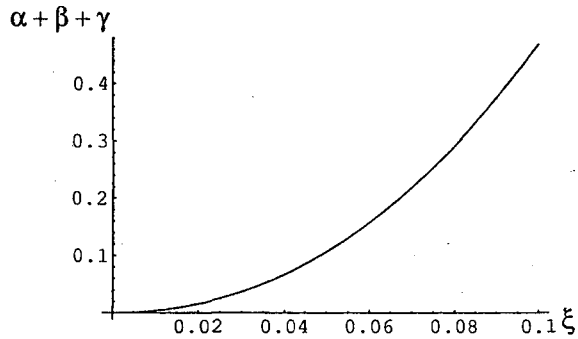

Figure 5: Sum of the Angles α, β, γ in the ncSM illustrating that the unitarity triangle does not close:

moment $\vec{D}$ is a directional quantity, so for an elementary particle it must transform like the spin $\vec{J}$, the only available directional quantum number. The interation with an external electric field $\vec{E}$ is $\vec{J} \cdot \vec{E}$ which is therefore CP-odd. The presence of an *edm* for a particle ψ implies an interaction with the electromagnetic field strength $F^{\mu\nu}$ in the Lagrangian of the form

$$O_{edm} = -(i/2)\overline{\psi}\gamma_5\sigma_{\mu\nu}\psi F^{\mu\nu}$$

In the SM this operator is absent at tree level and even at one loop due to a cancellation of the CKM phases. For the electron, moreover, the *edm* (d_e) vanishes at two loops and the three-loop prediction is miniscule, of order $10^{-50}e\ cm$ [46]. For the neutron *edm* (d_n), gluon interactions can give rise to a two-loop contribution which is $\mathcal{O}(10^{-33})e\ cm$. Upper limits from experiments exist: $d_e \leq 4.3 \cdot 10^{-27}e\ cm$ [47], $d_n \leq 6.3 \cdot 10^{-26}e\ cm$ [48].

Since the SM predictions of *edm*s are almost zero, we might expect that new sources of CP violating physics from noncommutative geometry would be observable. The noncommutative geometry provides in addition a simple explanation for this type of CP violation: the directional sense of $\vec{D}$ derives from the different amounts of noncommutivity in different directions (*i.e.* $D_i \propto \epsilon_{ijk}\theta^{jk}$) and the size of the *edm*, classically proportional to the spatial extent of a charge distribution, is likewise in noncommutative geometry proportional to $|\theta|$, the inherent "uncertainty" of space. However, the effects of noncommutative geometry are proportional to the typical momentum involved, which for an electron *edm* observation is very small. Even if the electrons under observation had energies $\sim MeV$, the expected dipole moment would be

$$d_e \sim e\left|p^2\theta\right| G_F m_e/16\pi^2 \approx 10^{-33}\xi^2\ e \cdot cm \tag{30}$$

which gives only a very weak upper bound: $\xi < 10^4$. Since the phenomenologically interesting values of ξ from the K- and B-meson sectors are well below this bound, we conclude that the *edm*s do not lead to any useful constraints on noncommutative geometry.

4 Constraints from g − 2 of the Muon

We saw above that the electron *edm*, despite being constrained by very precisely measured bounds, does not meaningfully constrain the amount of noncommutivity in low enegy physics since the typical momentum with which the electron moves in an *edm* experiment is too small compared with even the smallest noncommutivity scale permitted by K-physics ($\Lambda \approx 2\ TeV$): $p_e^2\theta \ll 10^{-13}$.

The situation might improve if we were considering the muon *edm* in an experiment using relativistic muons, however the experimental bound here is weaker: $d_\mu < 1.05 \cdot 10^{-18} e\ cm$ [49].

The recent measurement of the anomalous magnetic moment of the muon [50], a_μ, although not a CP violating observable, does however provide an interesting constraint on the ncSM. Experiments dedicated to a_μ have undergone continual refinement (for history and experimental details, see [49], [51]) to the point where a_μ is now very precisely known:

$$a_\mu^{expt} = 11659202(14) \cdot 10^{-10} \tag{31}$$

The experimental technique employs muons trapped in a storage ring. A uniform magnetic field B is applied perpendicular to the orbit of the muons; hence the muon spin will precess. The signal is a discrepancy between the observed precession and cyclotron frequencies.

Precession of the muon spin is determined indirectly from the decay $\mu \to e\ \overline{\nu}_e\ \nu_\mu$. Electrons emerge from the decay vertex with a characteristic angular distribution which in the SM has the following form in the rest frame of the muon:

$$dP(y,\phi) = n(y)(1 + A(y)cos(\phi))dyd(cos(\phi)) \tag{32}$$

where ϕ is the angle between the momentum of the electron and the spin of the muon, $y = 2p_e/m_\mu$ measures the fraction of the maximum available energy which the electron carries, and $n(y), A(y)$ are particular functions which peak at $y = 1$. The detectors (positioned along the perimeter of the ring) accept the passage of only the highest energy electrons in order to maximize the angular asymmetry in (32). In this way, the electron count rate is modulated at the frequency $a_\mu eB/(2\pi mc)$.

Although a_μ does receive a sizable contribution from noncommutative geometry, it is a *constant* contribution [27], *i.e.* the interaction with the external magnetic field $\Delta E \sim B_i\theta_{jk}\epsilon^{ijk}$ is independent of the muon spin, and therefore the experiment described above is not sensitive to this perturbation of a_μ. The effect of noncommutative geometry on this measurement does however enter in the manner in which the muon spin is measured in its decay. Specifically, the electron decay distribution (32) has a slightly different angular dependence due to the departure of the ncSM from the standard V-A theory of the weak interactions (see Figure 6). The electron distribution dP' in the ncSM differs from the SM (see Appendix for calculation):

$$\begin{aligned} dP'(y,\phi) &\approx n(y)\left(1 + A(y)(\hat{p}_e \cdot \vec{s}_\mu) + f(y)(\hat{p}_e \cdot \vec{s}_\mu)(\vec{\theta} \cdot \vec{s}_e) + \cdots\right) dyd\Omega \\ &\to n(1)\left(1 + A(1)cos(\phi) + f(1)cos^2(\phi)\,|\theta| + \cdots\right) dyd\Omega \\ \text{where} \quad & \left|\tfrac{f(1)}{A(1)}\right| \approx \tfrac{\alpha}{16\pi^2}\tfrac{p_\mu}{m_W}\xi \end{aligned} \tag{33}$$

The effect of noncommutative geometry is greater than one would naively expect as, for reasons of efficiency, the muons are stored at highly relativistic energies: $p_\mu \approx 3\ GeV$. Hence the ratio $\left|\frac{f(1)}{A(1)}\right| \approx 10^{-6}\xi$. However, the frequency is measured over many cycles and a more conservative estimate of the effective size of the noncommutative term is closer to $(10^{-7}\ to\ 10^{-8})\xi$ The angular distribution is therefore not a pure $cos(\phi)$ and we expect the measurement of the precession frequency to differ from the SM prediction at the level of 1 part in 10^8.

Currently, the discrepancy between the measured value of a_μ and the SM prediction is

$$a_\mu^{expt} - a_\mu^{SM} = 43(16) \cdot 10^{-10} \tag{34}$$

which imposes the constraint $\xi \leq 5 \cdot 10^{-2}$. This bound accomodates the values of ξ inferred from CP violating observables in section 3.1. We expect the value of ξ determined from a $g-2$ experiment

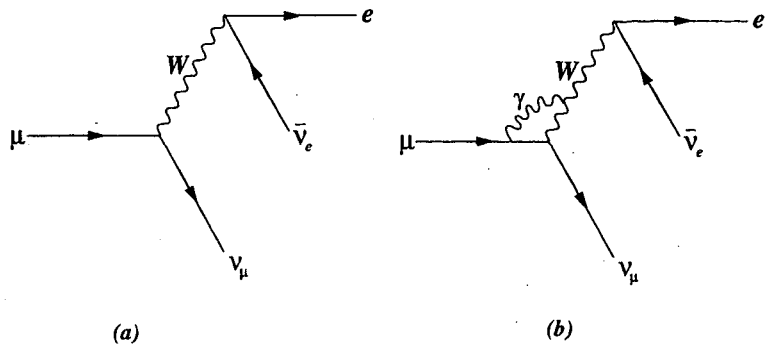

Figure 6: Contributions to muon decay (a) SM tree level (b) ncSM graph which upsets the electron's angular distribution

to be smaller than that from a K or B-physics experiment since the circulation of the muons at their cyclotron frequency introduces an additional averaging of the components of $\vec{\theta}$. For a storage ring located at an Earth lattitude of ψ degrees, there will be a $sin(\psi)$ suppression factor.

5 Conclusions

The Standard Model(SM) is a highly successful effective theory for energies below the weak scale $\sim$ 100 GeV, but it must eventually give way to a description of nature that includes gravity. Noncommutative geometry is one candidate for such a description, exhibiting some features of gravity such as nonlocality and space-time uncertainty.

In this paper we have considered the potential effects at low eneriges of a noncommutative geometry which sets in at some high scale Λ. Remarkably, for Λ in the TeV- range, noncommutative contributions to CP violating observables such as ϵ_K, ϵ'/ϵ, and $sin2\beta$ are competitive with the SM contributions. If $\Lambda \sim 2$ TeV, the predictions of these observables from noncommutative geometry is consistent with data. Moreover the recent 2.6 σ deviation between the SM prediction of $(g-2)$ of the muon and data is explained in the noncommutative scenario for this same value of Λ. These perturbative results in terms of the small parameter $\xi \equiv m_W/\Lambda$ are encouraging, but more work is needed in the treatment of the full, nonperturbative theory. Nonetheless, noncommutativity of the space-time coordinates offers a more physical interpretation of CP violation which, if correct, suggests interesting physics at TeV energies.

Acknowledgements

This work was supported in part by the Director, Office of Science, Office of High Energy and Nuclear Physics, of the U.S. Department of Energy under Contract DE-AC03-76SF00098.

A Feynman Rules in the NCSM

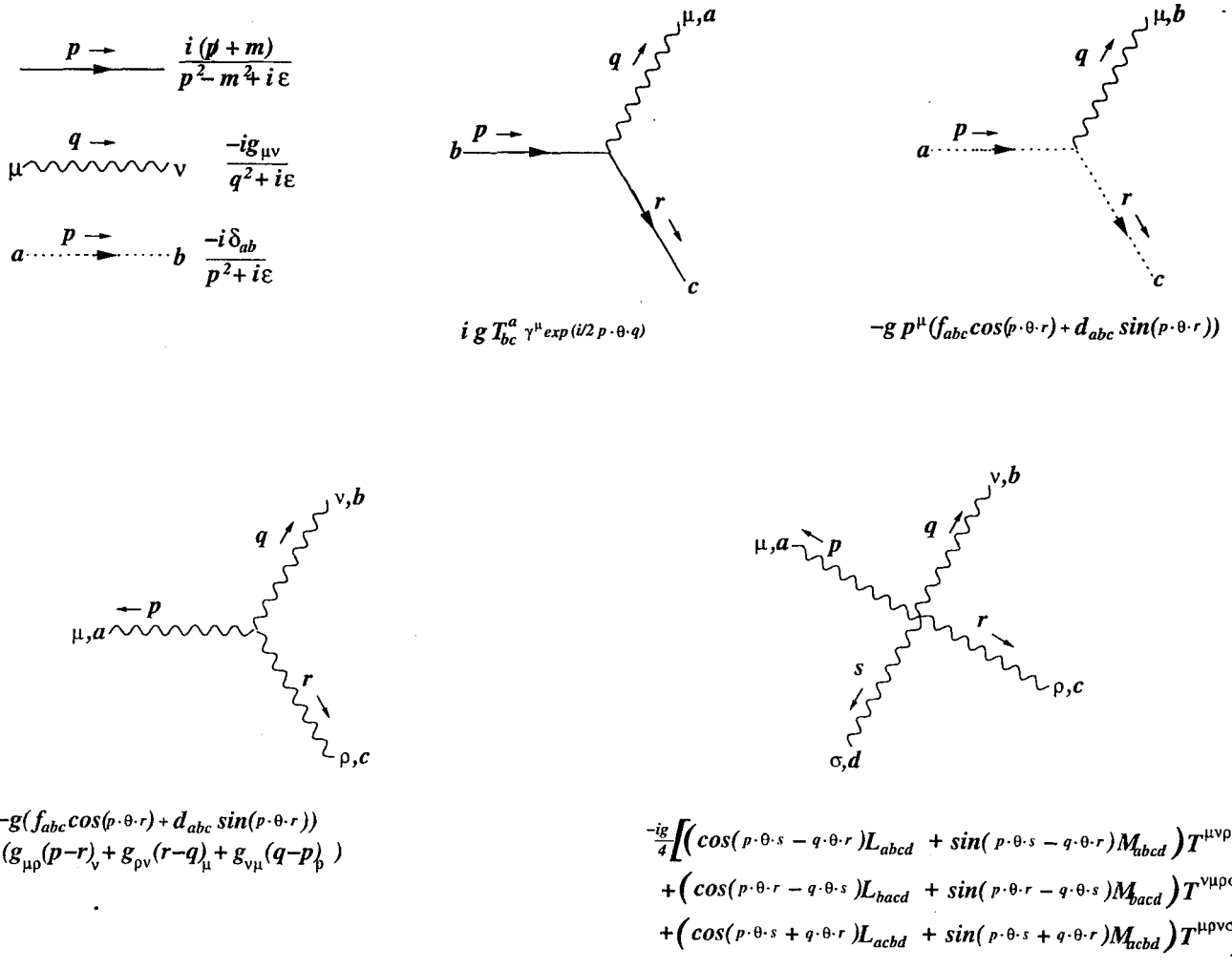

Figure 7: Feynman rules for fermions (solid lines), gauge particles (wavy lines), and ghosts (dotted lines). Notation: p, q, r, s Momenta μ, ν, ρ, σ Lorentz indices a, b, c, d gauge indices T^a_{bc} gauge generator f_{abc} structure constants for $SU(N)$: $[T_a, T_b] = f_{abc}T^c$ d_{abc} structure constants for $SU(N)$: $\{T_a, T_b\} = d_{abc}T^c + \frac{1}{N}\delta_{ab}$ $L_{abcd} \equiv d_{abe}d_{cde} + d_{ade}d_{cbe} - f_{abe}f_{cde} - f_{ade}f_{cbe}$ $M_{abcd} \equiv d_{abe}f_{cde} - d_{ade}f_{cbe} + f_{abe}d_{cde} - f_{ade}d_{bce}$ $T_{\mu\nu\rho\sigma} \equiv g_{\mu\nu}g_{\rho\sigma} + g_{\mu\sigma}g_{\nu\rho} - 2g_{\mu\rho}g_{\nu\sigma}$ For QED/Weak vertices, index 0 corresponds to a photon: $d_{0,i,j} = \delta_{ij}$, $d_{0,0,i} = 0$, and $d_{0,0,0} = 1$, $f_{0,a,b} = 0$.

B Kaon System

The loop function in (18) is given by

$$\begin{aligned} f(x) &\equiv \tfrac{x}{(1-x)^2}(1-\tfrac{11x}{4}+\tfrac{x^2}{4}-\tfrac{3x^2 ln(x)}{2(1-x)}) \\ f(x,y) &\equiv xy\left(\tfrac{-3}{4(1-x)(1-y)}+\tfrac{ln(y)(1-2y+\frac{y^2}{4})}{(y-x)(1-y)^2}+\tfrac{ln(x)(1-2x+\frac{x^2}{4})}{(x-y)(1-x)^2}\right) \end{aligned} \tag{35}$$

Numerically,

$$\begin{aligned} &f((m_t/m_W)^2) \approx 2.5 \\ &f((m_c/m_W)^2) \approx 2\cdot 10^{-4} \\ &f((m_c/m_W)^2,(m_t/m_W)^2) \approx 2\cdot 10^{-3} \end{aligned} \tag{36}$$

In the noncommutative case with $\eta = 0$, the imaginary part of the loop integral for the box graph becomes

$$\begin{aligned} &\int d^4k\ \overline{u}(p_1)\gamma_\mu(1-\gamma_5)(\not{p}_1-\not{k}+m_t)\gamma_\nu(1-\gamma_5)d(p_1-k) \\ &\times\overline{u}(p_2)\gamma_\mu(1-\gamma_5)(\not{k}-\not{p}_2+m_t)\gamma_\nu(1-\gamma_5)d(k-p_2) \\ &\times\tfrac{(\overline{V}_{td}\overline{V^*}_{ts})^2}{((p_2+k)^2-m_t^2)((p_1-k)^2-m_t^2)(k^2-m_W{}^2)^2} \end{aligned} \tag{37}$$

which in the high loop momentum limit ($k \gg p_1, p_2$) is approximately

$$i\lambda^3\rho\int_{m_W}^{M} d^4k\ \frac{(\frac{k^2m_t^4}{4m_W^4}+k^2-\frac{2m_t^4}{m_W^2})\,|k|\,|p_1\cdot\theta\cdot p_2|}{(k^2-m_t^2)^2(k^2-m_W^2)^2} \tag{38}$$

where we have introduced the cutoff $M \sim \Lambda$ explicitly since we don't know the theory at higher energies (taking this limit to infinity doesn't change the answer appreciably.) The imaginary part of the integral (38) is approximately

$$\Im(nc\ loop) \approx \frac{\lambda^3\rho}{m_W^2}\frac{m_K}{18m_W}\left(\frac{29\pi}{2}\xi^2+\frac{134\xi^3}{1+\xi^2}-\frac{20\xi^3}{4+\xi^2}\right) \tag{39}$$

where $\xi \approx \frac{m_W}{\Lambda}$.

C ϵ'/ϵ

Direct CP violation in the SM implies that two or more diagrams contribute to the kaon decay with disparate weak and strong phases. In noncommutative geometry, the vertex phases mimic a weak phase (*i.e.* we use the ncCKM matrix). To give an estimate for the effects of noncommutative geometry on ϵ'/ϵ, we consider a typical electroweak penguin loop integral. In the limit of high loop momentum, the penguin is characterized by the dimensionless number P_l

$$P_l \approx \int_m^M \frac{d^4k}{(2\pi)^4}\frac{i\ m_K\ sin(q\cdot\theta\cdot k)}{k^5} \tag{40}$$

where m is the mass of the heaviest particle in the loop and q is the typical momentum of the process $\sim m_t$ in a hadron machine. Switching to Euclidean space and performing the integral,

$$P_l \approx |m_K\theta q|\,[Ci(|\theta q\Lambda|)-Ci(|\theta qm|)]+\frac{sin(|\theta qm|)}{m}-\frac{sin(|\theta q\Lambda|)}{\Lambda} \tag{41}$$

where we take $M \sim \Lambda$. We use the cosine integral function which for small values of its argument is

$$Ci(x) \approx const. + ln(x) - \frac{x^2}{4} + \frac{x^4}{4!4} + \cdots \tag{42}$$

Taking the average mass $m \sim m_K$ for simplicity, we obtain in the limit of small $\xi \equiv \theta m_W^2$

$$P_l \approx 2\frac{m_K}{m_W}\xi^2 \; ln(\frac{m_W}{\xi m_K}) \tag{43}$$

as quoted in (23).

D $g-2$ of the muon

The squared matrix element for muon decay is (see, for example, [52])

$$|\mathcal{M}|^2 = \frac{G_F^2}{2} T_1 T_2 \tag{44}$$

where

$$\begin{aligned} T_1 &\equiv tr\left(\Lambda_e[\gamma_\alpha(1+\gamma_5)+\tilde{\theta}_\alpha]\Lambda_1[\gamma_\beta(1+\gamma_5)+\tilde{\theta}_\beta]\right) \\ T_2 &\equiv tr\left(\Lambda_2[\gamma^\alpha(1+\gamma_5)+\tilde{\theta}^\alpha]\Lambda_\mu[\gamma^\beta(1+\gamma_5)+\tilde{\theta}^\beta]\right) \\ \Lambda_i &\equiv \not{q}_i \\ \Lambda_e &\equiv \tfrac{1}{2}(\not{p}_e + m_e)(1-\gamma_5\not{s}_e) \\ \Lambda_\mu &\equiv \tfrac{1}{2}(\not{p}_\mu + m_\mu)(1-\gamma_5\not{s}_\mu) \end{aligned} \tag{45}$$

We neglect the neutrino masses $m_{1,2}$ and eventually the electron mass m_e as well. The vector object $\tilde{\theta}_\alpha$ comes from the 1-loop graph (Figure 6b) and is formally a function of the neutrino momenta $q_{1,2}$. We obtain

$$\left|\tilde{\theta}\right| \approx \frac{\alpha}{16\pi^2}\int^M d^4k \; \frac{k^2 \; sin(q\cdot\theta\cdot k)}{(k^2-m_\mu^2)(k^2-m_W^2)k^2} \tag{46}$$

where we use the explicit cutoff $M \sim \Lambda$. For high loop momenta, (46) becomes

$$\left|\tilde{\theta}\right| \approx \frac{\alpha}{16\pi^2}\int_{m_W}^M dk \; \frac{sin(q\cdot\theta\cdot k)}{k} \approx q\,|\theta\Lambda|\,\frac{\alpha}{16\pi^2} \approx \left(\frac{p_\mu}{m_W}\xi\right)\frac{\alpha}{16\pi^2} \approx 10^{-8} \tag{47}$$

We reduce $T_{1,2}$ to the form

$$\begin{aligned} T_1 &= (p_e - m_e s_e)^\rho q_1{}^\sigma \chi_{\rho\sigma\alpha\beta} + T_{1,\tilde{\theta}} \\ T_2 &= (p_\mu - m_\mu s_\mu)_\phi q_{2\gamma}\chi^{\phi\gamma\alpha\beta} + T_{2,\tilde{\theta}} \\ \chi_{\rho\sigma\alpha\beta} &\equiv g_{\rho\alpha}g_{\sigma\beta} + g_{\rho\beta}g_{\sigma\alpha} - g_{\rho\sigma}g_{\alpha\beta} - i\epsilon_{\rho\sigma\alpha\beta} \end{aligned} \tag{48}$$

The product of these two traces, neglecting the $\mathcal{O}(\theta)$ pieces, gives the usual angular distribution of electrons, as in (32). The $\mathcal{O}(\theta)$ pieces are

$$\begin{aligned} T_{1,\tilde{\theta}} &= p_e^\gamma s_e^\delta q_1^\eta \tilde{\theta}_\alpha \chi_{\gamma\delta\eta\beta} + p_e^\gamma s_e^\delta q_1^\eta \tilde{\theta}_\beta \chi'_{\gamma\delta\alpha\eta} \\ T_{2,\tilde{\theta}} &= p_{\mu\gamma} s_{\mu\delta} q_{2\eta}\tilde{\theta}^\alpha \chi^{\gamma\delta\eta\beta} + p_{\mu\gamma} s_{\mu\delta} q_{2\eta}\tilde{\theta}^\beta \chi'^{\gamma\delta\alpha\eta} + m_\mu(q_2^\beta\tilde{\theta}^\alpha + q_2^\alpha\tilde{\theta}^\beta) \\ \chi'_{\gamma\delta\alpha\eta} &\equiv g_{\delta\alpha}g_{\gamma\eta} + g_{\delta\eta}g_{\gamma\alpha} - g_{\gamma\delta}g_{\alpha\eta} + i\epsilon_{\gamma\delta\alpha\eta} \end{aligned} \tag{49}$$

After computing $|\mathcal{M}|^2$, it is necessary to integrate over the neutrino momenta $q_{1,2}$. Among the many terms that contribute to the final result, there will be some of the form $(\hat{p}_e \cdot \vec{s}_\mu)(\vec{\theta} \cdot \vec{s}_e)$.

For electrons close to the maximum possible energy ($y \sim 1$), the spin of the electron $\vec{s}_e$ is highly correlated with the spin of the muon $\vec{s}_\mu$ (for $y = 1$ the electron is emitted opposite to the left-handed neutrinos, hence $\vec{s}_e = -\vec{s}_\mu$). Terms of this type are essentially proportional to $(\hat{p}_e \cdot \vec{s}_\mu)(\vec{\theta} \cdot \vec{s}_\mu)$ which, as the muon spin precesses, gives a $cos^2(\phi)$ effect. Of course other terms in the product $T_1 T_2$ will contribute different angular effects, leading to deviations from the SM $cos(\phi)$ prediction at $\mathcal{O}(\theta)$.

References

[1] A. Connes, Noncommutative Geometry. New York: Academic Press, 1994

[2] M. Chaichian, A. Demichev,P. Presnajder,A. Tureanu, **hep-th/0007156**

[3] R. G. Cai and N. Ohta, JHEP 0010:036 (2000)

[4] E. Witten, Nuc.Phys **B 268**, 253 (1986); N. Seiberg and E. Witten, JHEP 9909:032 (1999)

[5] J. Madore, An introduction to noncommutative differential geometry and its physical applications. New York: Cambridge University Press, 1999

[6] A. Connes, Jour. Math. Phys. **41**, 3832 (2000)

[7] D. Kastler, Jour. Math. Phys. **41**, 3867 (2000)

[8] R. V. Mendes, Jour. Math. Phys. **41**, 156 (2000)

[9] J. C. Varilly, **physics/9709045**

[10] M. Dubois-Violette,J. Madore,R. Kerner, Jour. Math. Phys. **39**, 730 (1998)

[11] S. Doplicher,K. Fredenhagen, J. E. Roberts, Commun. Math. Phys. **172**, 187 (1995)

[12] S. Minwalla,M. Van Raamsdonk,N. Seiberg, JHEP 0002:020 (2000)

[13] M. Raamsdonk and N. Seiberg, JHEP 0003:035 (2000)

[14] A. Matusis,L. Susskind,N. Toumbas, JHEP 0012:002 (2000)

[15] H. Grosse,C. Klimcik,P. Presnajder, Commun. Math. Phys. **180**, 429 (1996)

[16] M. Chaichian, A. Demichev, P. Presnajder, Nuc. Phys. **B567**, 360 (2000)

[17] H. Grosse *et al.*, **hep-th/9602115**

[18] I. Y. Aref'eva,D. M. Belov,A. S. Koshelev, Phys. Lett **B476**, 431 (2000)

[19] M. Hayakawa, **hep-th/9912167**

[20] T. Krajewski and R. Wulkenhaar, Int. J. Mod. Phys. **A15**, 1011 (2000)

[21] A. Armoni, Nuc. Phys. **B593**, 229 (2001)

[22] L. Bonora and M. Salizzoni, Phys. Lett **B504**, 80 (2001)

[23] C. Brouder and A. Frabetti, **hep-th/0011161**

[24] J. Madore,S .Schraml,P. Schupp,J. Wess, Eur. Phys. J. **C16**, 161 (2000)

[25] J. L. Hewett,F. J. Petriello,T. G. Rizzo, **hep-ph/0010354**

[26] M. Chaichian,M. M. Sheikh-Jabbari,A. Tureanu, Phys. Rev. Lett **86**, 2716 (2001)

[27] I. F. Riad and M. M. Sheikh-Jabbari, JHEP 0008:045 (2000)

[28] J. Schwinger, Phys. Rev. **76**,790 (1949)

[29] R. J. Crewther *et al.*, Phys. Lett. **88B**, 123 (1979). Errata **91B**, 487 (1980)

[30] M. M. Sheikh-Jabbari, Phys. Rev. Lett **84**,5265 (2000)

[31] M. M. Sheikh-Jabbari, JHEP 9906:015 (1999)

[32] L. Wolfenstein, Phys. Rev. Lett **51**,1945 (1983)

[33] D. Atwood, S. Bar-Shalom,G. Eilam,A. Soni, **hep-ph/0006032**

[34] D. E. Groom *et al.*, Eur. Phys. J. **C15** 1 (2000)

[35] R. Adler *et al.*, Nuc. Instrum. Meth. **A379** 76 (1996)

[36] O. Yavas,A. K. Ciftci, S. Sultansoy, **hep-ex/0005035**

[37] S. Bertolucci *et al.*, Int. J. Mod. Phys. A **15S1** 132 (2000)

[38] S. Bertolini, **hep-ph/0101212**

[39] S. Bertolini,M. Fabbrichesi,J. O. Eeg, Rev. Mod. Phys. **72**,65 (2000)

[40] R. Barate *et al.*, Phys. Lett. **B492** 259 (2000)

[41] B. Aubert *et al.*, **hep-ex/0102030**

[42] A. Abashian *et al.*,**hep-ex/0102018**

[43] T. Affolder *et al.*, Phys. Rev. **D61** 072005 (2000)

[44] S. Mele, **hep-ph/0103040**

[45] R. Culbertson *et al.*, **hep-ph/0008070**

[46] J. Donoghue, Phys. Rev. **D18** 1632 (1978)

[47] E. D. Commins,S. B. Ross,D. DeMille,B. C. Regan, Phys. Rev. **A50** 2960 (1994)

[48] P. G. Harris *et al.*, Phys. Rev. Lett **82**,904 (1999)

[49] F. J. M Farley and E. Picasso, Quantum Electrodynamics, ed. T. Kinoshita. Singapore: World Scientific, 1990

[50] H. N. Brown, *et al.*, Phys. Rev. Lett **86**,2227 (2001)

[51] B. Lee Roberts, Int. J. Mod. Phys. A **15S1**,386 (2000)

[52] E. D. Commins, Weak Interactions. New York: McGraw-Hill,1973

Ernest Orlando Lawrence Berkeley National Laboratory
One Cyclotron Road | Berkeley, California 94720

Prepared for the U.S. Department of Energy under Contract No. DE-AC03-76SF00098